NUMERICAL METHOD FOR SOLVING A PREMIXED LAMINAR FLAME*

ZHONG XI-CHANG (钟锡昌)

(Computing Center, Academia Sinica)

Abstract

A splitting-up method, which splits the chemical kinetic terms from the flow terms, is presented to solve time-dependent, one-dimensional, laminar, premixed flame problems. An example for studying the development of an ozone decomposition flame is calculated. A movable boundary technique is adopted, so that the number of grid points can be significantly reduced. Special care is taken to maintain the accuracy of the solution. The results are checked in many ways. All checks show that the present method is satisfactory.

Nomenclature

x space coordinate
t time coordinate
p pressure
ρ density of fluid mixture
T temperature
y_i mass fraction of the i-th species
v velocity of fluid mixture
R universal gas constant
C_p specific heat capacity at constant pressure of the fluid mixture
C_{p_i} specific heat capacity at constant pressure of the i-th species
ω_i rate of production of i-th species
M_i molecular weight of i-th species
D_i binary diffusion coefficient for the i-th species
λ thermal conductivity
h_i enthalpy of i-th species
h_0^i standard enthalpy of formation of i-th species

1. Introduction

More and more attention is paid to combustion problems not only by engineers but also by mathematicians, because a number of interesting and difficult problems occur. For example, a premixed flame problem will reduce to a typical reaction-diffusion equation.

It is well known that in a premixed combustible fluid mixture a steady flame

* Received August 26, 1982.

will be developed when it is ignited. This fact has been proved theoretically for a simple chemical reaction model. There have been many works on studying the configuration of a laminar, premixed flame. These works have essentially followed two different approaches. One is the steady-state approach in which the problem to be solved is reduced to a two-point boundary value problem of ordinary differential equations. The other is the time-dependent approach in which the full time-dependent equations with proper boundary and initial conditions are treated. In this paper our attention is focused on the latter approach.

Since the combustion processes are highly exothermic, chemical reaction processes and there exist a number of vastly differing time scales, numerical solutions will suffer from a number of difficulties. One is stiffness. With this in mind a splitting-up method is presented, which splits the chemical kinetic terms from the fluid mechanical terms. We think it might ameliorate some of the difficulties.

Generally speaking, the region of calculation must be taken large enough, therefore a large amount of grid points must be taken. Obviously it is costly. In order to reduce grid points a movable boundary technique is adopted.

Special care of error control is taken to maintain the accuracy of the solutions.

For comparison of the results obtained by the present methods with published results an example for an ozone decomposition flame is calculated. The results are also checked in many ways. The comparison and check show that the present methods are satisfactory.

2. Formulation of the Problem

2.1 *Governing Equations*

We consider one-dimensional flow and neglect the effects of radiative heat transfer and thermal and pressure diffusion. The governing equations are as follows.

Continuity

$$\frac{\partial \rho}{\partial t}+\frac{\partial(\rho u)}{\partial x}=0. \tag{2.1}$$

Conservation of momentum

$$\rho \frac{\partial u}{\partial t}+\rho u \frac{\partial u}{\partial x}=-\frac{\partial p}{\partial x}+\frac{\partial}{\partial x}\left[\left(\mu+\frac{4}{3}\varkappa\right)\frac{\partial u}{\partial x}\right]. \tag{2.2}$$

Conservation of species

$$\rho \frac{\partial y_i}{\partial t}+\rho u \frac{\partial y_i}{\partial x}=\frac{\partial}{\partial x}\left(\rho D_i \frac{\partial y_i}{\partial x}\right)+\omega_i. \tag{2.3}$$

Conservation of energy

$$\rho C_p \frac{\partial T}{\partial t}+\rho C_p u \frac{\partial T}{\partial x}=\frac{\partial p}{\partial t}+u \frac{\partial p}{\partial x}+\left(\mu+\frac{4}{3}\varkappa\right)\left(\frac{\partial u}{\partial x}\right)^2+\frac{\partial}{\partial x}\left(\lambda \frac{\partial T}{\partial x}\right)$$
$$-\sum_{i=1}^{N}\omega_i h_i-\sum_{i=1}^{N}\rho D_i C_{p_i}\frac{\partial y_i}{\partial x}\frac{\partial T}{\partial x}, \tag{2.4}$$

and equation of state

$$\rho=\frac{p}{\left(\Sigma\frac{y_i}{M_i}\right)RT}. \tag{2.5}$$

The variables appearing in these equations have their usual meaning as listed in nomenclature. In order to simplify these equations further, the effect of viscosity is assumed to be negligible and fluid velocity is assumed to be small compared to the speed of sound. From the latter we can integrate equation (2.2) and obtain the following condition.

$$p=p_0=\text{const.} \tag{2.6}$$

Then the equations (2.1)—(2.5) are simplified into

$$\frac{\partial\rho}{\partial t}+\frac{\partial(\rho u)}{\partial x}=0, \tag{2.7}$$

$$\frac{\partial y_i}{\partial t}+u\frac{\partial y_i}{\partial x}=\frac{1}{\rho}\frac{\partial}{\partial x}\left(\rho D_i\frac{\partial y_i}{\partial x}\right)+\frac{\omega_i}{\rho}, \tag{2.8}$$

$$\frac{\partial T}{\partial t}+u\frac{\partial T}{\partial x}=\frac{1}{\rho C_p}\frac{\partial}{\partial x}\left(\lambda\frac{\partial T}{\partial x}\right)-\frac{1}{\rho C_p}\sum_{i=1}^{N}\omega_i h_i-\left(\sum_{i=1}^{N}\rho D_i C_{p_i}\frac{\partial y_i}{\partial x}\right)\frac{\partial T}{\partial x}, \tag{2.9}$$

$$\rho=\frac{p_0}{\left(\Sigma\frac{y_i}{M_i}\right)RT}. \tag{2.10}$$

It is convenient to introduce a Lagrangian coordinate ψ,

$$\psi(x,\ t)=\int_0^x\rho(x,\ t)\,dx \tag{2.11}$$

Under these coordinates, the continuity equation (2.7) is identically satisfied, because

$$\frac{\partial\psi}{\partial x}=\rho,$$

$$\frac{\partial\psi}{\partial t}=\int_0^x\frac{\partial\rho(x,\ t)}{\partial t}\,dx=-\int_0^x\frac{\partial}{\partial x}(\rho u)\,dx=-\rho u+m_0,$$

where $m_0=\rho u|_{x=0}$. Since

$$\frac{\partial}{\partial x}=\frac{\partial\psi}{\partial x}\frac{\partial}{\partial\psi}=\rho\frac{\partial}{\partial\psi},$$

$$\frac{\partial}{\partial t}=\frac{\partial\psi}{\partial t}\frac{\partial}{\partial\psi}+\frac{\partial}{\partial t}=(-\rho u+m_0)\frac{\partial}{\partial\psi}+\frac{\partial}{\partial t},$$

the remaining equations become

$$\frac{\partial y_i}{\partial t}+m_0\frac{\partial y_i}{\partial\psi}=\frac{\partial}{\partial\psi}\left(\rho^2 D_i\frac{\partial y_i}{\partial\psi}\right)+\frac{\omega_i}{\rho}, \tag{2.12}$$

$$\frac{\partial T}{\partial t}+m_0\frac{\partial T}{\partial\psi}=\frac{1}{C_p}\frac{\partial}{\partial\psi}\left(\rho\lambda\frac{\partial T}{\partial\psi}\right)-\sum_{i=1}^{N}\omega_i h_i-\sum_{i=1}^{N}\frac{C_{p_i}}{C_p}\rho^2 D_i\frac{\partial y_i}{\partial\psi}\frac{\partial T}{\partial\psi}. \tag{2.13}$$

By introducing the following nondimensional variables:

$$\rho^* = \frac{\rho}{\rho_\infty}, \qquad T^* = \frac{T}{T_\infty},$$

$$D_i^* = \frac{D_i}{D_\infty}, \qquad \lambda^* = \frac{\lambda}{\lambda_\infty},$$

$$C_p^* = \frac{C_p}{C_{p_\infty}}, \qquad C_{p_i}^* = \frac{C_{p_i}}{C_{p_\infty}},$$

$$h^* = \frac{h}{C_{p_\infty} T_\infty}, \qquad M_i^* = \frac{M_i}{M_\infty},$$

$$t^* = \frac{t}{t_\infty}, \qquad \omega_i^* = \frac{\omega_i t_\infty}{\rho_\infty},$$

$$x^* = \frac{x}{l_\infty}, \qquad l_\infty = \sqrt{\frac{\lambda_\infty t_\infty}{\rho_\infty C_{p_\infty}}},$$

$$\psi^* = \frac{\psi}{\psi_\infty}, \qquad \psi_\infty = \rho_\infty l_\infty = \sqrt{\frac{\rho_\infty \lambda_\infty t_\infty}{C_{p_\infty}}},$$

the equations can be nondimensionalized as

$$\frac{\partial y_i}{\partial t} + m_0 \frac{\partial y_i}{\partial \psi} = (L_\infty)^{-1} \frac{\partial}{\partial \psi}\left(\rho^2 D_i \frac{\partial y_i}{\partial \psi}\right) + \frac{\omega_i}{\rho}, \tag{2.14}$$

$$\frac{\partial T}{\partial t} + m_0 \frac{\partial T}{\partial \psi} = \frac{1}{C_p} \frac{\partial}{\partial \psi}\left(\rho\lambda \frac{\partial T}{\partial \psi}\right) - \frac{1}{\rho C_p} \sum_{i=1}^{N} h_i \omega_i - (L_\infty)^{-1} \sum_{i=1}^{N} \frac{C_{p_i}}{C_p} \rho^2 D_i \frac{\partial y_i}{\partial \psi} \frac{\partial T}{\partial \psi}, \tag{2.15}$$

where

$$L_\infty = \frac{\lambda_\infty}{\rho_\infty D_\infty C_{p_\infty}}$$

is a characteristic Lewis number, and ρ_∞, T_∞, D_∞, λ_∞, C_{p_∞} and M_∞ are some characteristic values of density, temperature, mass diffusivity, heat conductivity, specific heat capacity, and molecular weight, respectively. For simplicity, the superscript star is omitted in the above equations.

2.2 *Initial and boundary conditions*

The equations (2.14)—(2.15) are a parabolic system; thus boundary and initial conditions are required. In this paper we consider the propagation of a premixed flame. So we can specify the boundary conditions in the following way. At the burned boundary the burned values are taken and at the unburned boundary the unburned values are taken, i. e.

$$T = T_b, \quad y_i = y_{ib}, \qquad \text{at burned boundary}$$

$$T = T_u, \quad y_i = y_{iu}. \qquad \text{at unburned boundary}$$

The unburned and burned values must satisfy some conditions, which depend on what model is assumed. For example, in this paper we assume that the flame is an adiabatic flame and the burned values satisfy chemically equilibrium equations.

The initial conditions are specified as a step function, i. e.

$$T(\psi, 0)=\begin{cases} T_u \\ T_b \end{cases} \text{for} \begin{matrix} \psi>\psi_o, \\ \psi\leqslant\psi_o; \end{matrix}$$
$$y_i(\psi, 0)=\begin{cases} y_{iu} \\ y_{ib} \end{cases} \text{for} \begin{matrix} \psi>\psi_o, \\ \psi\leqslant\psi_o, \end{matrix} \tag{2.16}$$

where ψ_o is a given value.

2.3 *Chemical Kinetic Formulation*

The elementary chemical reactions are expressed as

$$\sum_{i=1}^{N} v'_{m,i}x_i \rightleftharpoons \sum_{i=1}^{N} v''_{m,i}x_i,\ m=1, 2, \cdots, M. \tag{2.17}$$

The rate of production ω_i of the i-th species appearing in equations (2.12), (2.13) is given by the law of mass action.

$$\omega_i=\sum_{m=1}^{M}(v''_{m,i}-v'_{m,i})\,M_i\left[k'_m\prod_{i=1}^{N}c_i v'_{m,i}-k^b_m\prod_{i=1}^{N}c_i v''_{m,i}\right], \tag{2.18}$$

where $v'_{m,i}$ and $v''_{m,i}$ are the stoochastic coefficients of the species i, $i=1, \cdots, N$, appearing in a reactant and product in the reversible reaction m, $m=1, 2, \cdots, M$. c_i are the moles per unit volume of species i and related to the mass fraction by

$$c_i=\frac{\rho}{M_i}y_i. \tag{2.19}$$

The specific rate constants for forward and backward mode of reaction m are usually given by the following expression.

$$k^f_m=B^f_m T^{s^f_m}e^{-E^f_m/RT},$$
$$B^f_m,\ s^f_m,\ E^f_m=\text{const.} \tag{2.20}$$

k^b_m has a similar expression. The constants E^f_m and E^b_m are the activation energy of the forward and backward mode of reaction m, respectively. In terms of nondimensional variables ω_i in the equation (2.14) is expressed as

$$\frac{\omega^*_i}{\rho^*}=\sum_{i=1}^{M}M^*_i(v''_{m,i}-v'_{m,i})\left[k^{f^*}_m\rho^{*\alpha_m-1}\prod_{i=1}^{N}\left(\frac{y_i}{M_i}\right)^{v'_{m,i}}-k^{b^*}_m\rho^{*\beta_m-1}\prod_{i=1}^{N}\left(\frac{y_i}{M_i}\right)^{v''_{m,i}}\right], \tag{2.21}$$

where the superscript star refers to the nondimensional variable and

$$\alpha_m=\sum_{i=1}^{N}v'_{m,i},\quad \beta_m=\sum_{i=1}^{N}v''_{m,i},$$
$$k^{f^*}_m=k^f_m t_\infty\left(\frac{\rho_\infty}{M_\infty}\right)^{\alpha_m-1}, \tag{2.22}$$
$$k^{b^*}_m=k^b_m t_\infty\left(\frac{\rho_\infty}{M_\infty}\right)^{\beta_m-1}.$$

Correspondingly, in the equation (2.15)

$$\frac{1}{\rho^*}\sum_{i=1}^{N}h^*_i\omega^*_i=\sum_{m=1}^{M}\sum_{i=1}^{N}\left(\frac{h^f_0}{M_i C_{p_\infty}T_\infty}+C^*_{p_i}(T^*-T^*_0)\,M^*_i(v''_{m,i}-v'_{m,i})\right)$$
$$\times\left[k^{f^*}_m\rho^{*\alpha_m-1}\prod_{i=1}^{N}\left(\frac{y_i}{M_i}\right)^{v'_{m,i}}-k^{b^*}_m\rho^{*\beta_m-1}\prod_{i=1}^{N}\left(\frac{y_i}{M_i}\right)^{v''_{m,i}}\right]. \tag{2.23}$$

3. Numerical Method

3.1 *Coordinate Transformation*

Strictly speaking, the infinite boundary must be considered, but it is impossible and unnecessary in practice. In general one can take a value, ψ large enough to allow the full development of the flame before any effect could be felt there. However it is costly to do so. In order to reduce grid points, it is effective to adopt the movable boundary and to introduce the following coordinate transformation:

$$\begin{cases} \xi = \dfrac{\psi - \psi_b(t)}{\psi_u(t) - \psi_b(t)} = \dfrac{\psi - \psi_b(t)}{\varepsilon(t)}, \\ t = t, \end{cases}$$

where ψ_b, ψ_u represent the burned and unburned values, ψ, respectively. Since

$$\frac{\partial}{\partial t} = \frac{\partial}{\partial \xi}\frac{\partial \xi}{\partial t} + \frac{\partial}{\partial t} = \frac{\partial}{\partial t} - \frac{\xi(\dot{\psi}_u - \dot{\psi}_b) + \dot{\psi}_b}{\varepsilon}\frac{\partial}{\partial \xi},$$

$$\frac{\partial}{\partial \psi} = \frac{1}{\varepsilon}\frac{\partial}{\partial \xi}$$

the equations (2.14)—(2.15) become

$$\frac{\partial y_i}{\partial t} + \frac{m_0 + b}{\varepsilon}\frac{\partial y_i}{\partial \xi} = \frac{1}{L_\infty \varepsilon^2}\frac{\partial}{\partial \xi}\left(\rho^2 D_i \frac{\partial y_i}{\partial \xi}\right) + \frac{\omega_i}{\rho}, \tag{3.1}$$

$$\frac{\partial T}{\partial t} + \frac{m_0 + b}{\varepsilon}\frac{\partial T}{\partial \xi} = \frac{1}{C_p \varepsilon^2}\frac{\partial}{\partial \xi}\left(\rho\lambda \frac{\partial T}{\partial \xi}\right) - \frac{1}{\rho C_p}\sum_{i=1}^{N}\omega_i h_i - \frac{1}{L_\infty \varepsilon^2}\sum_{i=1}^{N}\frac{C_{p_i}}{C_p}\rho^2 D_i \frac{\partial y_i}{\partial \xi}\frac{\partial T}{\partial \xi}, \tag{3.2}$$

where $b = -\xi(\dot{\psi}_u - \dot{\psi}_b) + \dot{\psi}_b$ and the dot represents the derivative with respect to t.

In order to solve the equations (3.1)—(3.2), a splitting-up method is presented.

3.2 *Splitting-up Method*

The system of equations (3.1) — (3.2) is usually stiff and the solution frequently has rapid transients. In other words, there are a number of time scales and these scales vary widely. For example, in the vicinity of the flame, the chemical reactions are quite rapid, compared with the fluid mechanical scale and among the chemical reactions some may be quite faster than others. The splitting-up method could allow one to use different step sizes according to different time scales, e. g. one large step size can be used to advance the slowly varying terms while several smaller step sizes can be taken on the faster terms. For simplicity we rewrite the equations (3.1)—(3.2) as

$$\frac{\partial f}{\partial t} = a\frac{\partial f}{\partial \xi} + d\frac{\partial}{\partial \xi}\left(\eta\frac{\partial f}{\partial \xi}\right) + g. \tag{3.3}$$

We split equation (3.3) into two parts which group the fluid mechanics and chemical kinetic terms.

$$\frac{\partial f}{\partial t} = a\frac{\partial f}{\partial \xi} + d\frac{\partial}{\partial \xi}\left(\eta\frac{\partial f}{\partial \eta}\right), \tag{3.4}$$

$$\frac{\partial f}{\partial t}=g. \tag{3.5}$$

Since equation (3.4) is parabolic, we use the following implicit finite difference scheme:

$$\frac{\bar{f}_j^{i+1}-f_j^i}{\Delta t}=\frac{a_j}{2\Delta\xi}(\bar{f}_{j+1}^{i+1}-\bar{f}_{j-1}^{i+1})$$

$$+\frac{d_j}{\Delta\xi^2}[\eta_{j+1/2}\bar{f}_{j+1}^{i+1}-(\eta_{j+1/2}+\eta_{j-1/2})\bar{f}_j^{i+1}+\eta_{j-1/2}\bar{f}_{j-1}^{i+1}], \tag{3.6}$$

where superscripts represent time location and subscripts denote space location, and

$$\eta_{j+1/2}=\frac{1}{2}(\eta_{j+1}+\eta_j), \qquad \eta_{j-1/2}=\frac{1}{2}(\eta_j+\eta_{j-1}). \tag{3.7}$$

Obviously, the equation (3.6) is a tridiagonal system. So the solutions for any $\bar{f}$ and all j can be accomplished with a tridiagonal matrix algorithm.

Having obtained the solution for the first part of the split, we may turn our attention to the equation (3.5). The solutions $\bar{f}_j^{i+1}$ can be thought of as predicated intermediate values of the solution, and are used as the initial conditions of the equation (3.5). Since g contains no spatial derivatives equation (3.5) is a system of ordinary differential equations at each grid j. Usually the equation is stiff, so some effective stiff methods such as the Hindmarsh-Gear package can be used.

In order to improve the accuracy and efficiency of the calculation, a symmetric split operator is used. Let L_D be the operator providing a predicated value of $\bar{f}_j^{i+1}$ and L_C be the operator that obtains a correction of the first step. The following operator is used to advance the solution from t to $t+2\Delta t$:

$$f_j^{i+2}=L_D L_C L_C L_D f_j^i. \tag{3.8}$$

3.3 *Error Control*

In calculating the nonlinear terms a, d, η, g of equations (3.6) and (3.8) are linearized and evaluated explicitly. In order to control error the following approach is taken. We take two steps of $\Delta t/2$ and one step of Δt; then compare the solutions at $t+\Delta t$. Let

$$e=\max_j\left[\frac{|\bar{f}_j^{i+1(1)}-\bar{f}_j^{i+1(2)}|}{\max|\bar{f}_j^{i+1(2)}|}\right], \tag{3.9}$$

where superscripts (1), (2) refer to the number of steps. Whether the step size is increased or decreased depends on whether e is less than or greater than E. E is an error tolerance and is specified beforehand. If the convergence has been reached (i. e. $e<E$), $\bar{f}_j^{i+1(2)}$ is taken as the solution at $t+\Delta t$.

3.4 *Movable Boundary Technique*

As previously pointed out, if the boundary is fixed, a large value of ψ must be taken. Thus it is computationally costly. It is naturally desirable that the computational domain be confined to such a region that it always contains the flame and it is as small as possible. It is well known that in a premixed combustible fluid mixture a steady flame will be established after ignition. In other words, the flame will propagate through the combustible fluid with a constant velocity. In view of this fact, the movable boundaries could be used. Moreover, the moving velocity could be taken to be the same as the velocity of the flame. Let $\dot{\psi}_u$, $\dot{\psi}_b$, S_u represent

the moving velocities of the unburned boundary, the burned boundary, and the flame, respectively. Then the boundary values of ψ are obtained by integrating

$$\frac{d\psi_u}{dt} = -\dot{\psi}_u,$$

$$\frac{d\psi_b}{dt} = -\dot{\psi}_b. \tag{3.10}$$

The flame velocity based on the density of the unburned mixture can be evaluated by means of the mass conservation principle. That is, the net mass production rate of species i, inside a control volume (which is large compared to the thickness of the flame), must be equal to the mass rate of outflow of species i. The resulting equation in terms of ψ is

$$S_{u_i} = \int_{\psi_u}^{\psi_b} \frac{\omega_i}{\rho}\, d\psi / \rho_u (y_{ib} - y_{iu}). \tag{3.11}$$

In principle, any of the chemical species can be used to compute the flame velocity, because all these computed flame velocities should be identical. But in practice, owing to the numerical error there are some differences between these velocities. In our calculation one of them is taken and the other is used to check the accuracy of the calculation.

In order that the calculated region can be automatically confined to where significant changes occur, the grid interval is allowed to expand or contract. The way to do so is as follows. At the beginning, we use

$$\dot{\psi}_u = \tilde{\dot{\psi}}_{ui}\left[\frac{y_{iu} - y_{iuu}}{y_{iu} - y_{ib}} \times \delta\right]^{\alpha},$$

$$\tilde{\dot{\psi}}_b = \tilde{\dot{\psi}}_{ui}\left[2 - \left\{\left(\frac{y_{ib} - y_{ibb}}{y_{ib} - y_{iu}}\right) \times \delta\right\}^{\alpha}\right], \tag{3.12}$$

where $$\tilde{\dot{\psi}}_{ui} = -\int_{\psi_u}^{\psi_b} \frac{\omega_i}{\rho}\, d\psi / (y_{ib} - y_{iu}),$$

and δ, α are some constants (e. g. $\delta = 100$, $\alpha = 0.1$). Subscripts uu, bb represent some grid points near the unburned and burned boundaries, respectively. After the calculation proceeds for certain time steps we turn to use

$$\dot{\psi}_u = \dot{\psi}_b = -\rho_u s_u = -\frac{\int_{\psi_u}^{\psi_b} \frac{\omega_i}{\rho}\, d\psi}{y_{ib} - y_{iu}}. \tag{3.13}$$

The reason for doing so is that we found it was not easy for the flame velocity to be stable if only the formulas (3.12) are used.

4. Example of Calculation

The method described above is applied to calculate the structure of an ozone decomposition flame. In order to compare the results with the published results, the following nonessential approximations were made.

$$D_1 = D_2 = \cdots = D_i = D \quad \text{and} \quad \rho^2 D = \text{const.} = \rho_\infty^2 D_\infty,$$

$$\rho\lambda = \text{const.} = \rho_\infty \lambda_\infty,$$

$$C_{p_1}=C_{p_2}=\cdots=C_{p_i}=C_p=C_{p_N}.$$

The reaction mechanism for the ozone decomposition consists of seven reversible reactions.

$$O_3+x \underset{k_1^b}{\overset{k_1^f}{\rightleftharpoons}} O_2+O+x, \tag{4.1}$$

$$O+O_3 \underset{k_2^b}{\overset{k_2^f}{\rightleftharpoons}} 2O_2, \tag{4.2}$$

$$O_2+x \underset{k_3^b}{\overset{k_3^f}{\rightleftharpoons}} 2O+x, \tag{4.3}$$

where x represents any of the three species O, O_2, O_3.

Below we illustrate how to determine the boundary conditions. At unburned boundary a combustible mixture of 75% O_2 and 25% O_3 (by volume) at a temperature of 300°K are assumed. That is,

$$y_{1u}=0,\quad y_{2u}=\frac{2}{3},\ y_{3u}=\frac{1}{3},\quad T_u=300°\mathrm{K}, \tag{4.4}$$

The burned values can be determined by the unburned values. Between these values some conditions must be satisfied. In this case, they are

conservation of total enthalphy

$$C_pT_b-C_pT_u+y_{1b}h_0^{(1)}=y_{3u}h_0^{(3)}, \tag{4.5}$$

and chemical equilibrium equation

$$\left(\frac{\rho_b y_{1b}}{M_1}\right)^2=\frac{k_3^f}{k^b}\frac{\rho_b y_{2b}}{M_2}. \tag{4.6}$$

The equations (4.5), (4.6) are a system of nonlinear equations. The Newton iteration method is used. The solutions are

$$\begin{aligned} &y_{1b}=0.1259\times10^{-7},\ y_{2b}=1-0.1259\times10^{-7},\\ &y_{3b}=0,\quad T_b=1246.9°\mathrm{K}. \end{aligned} \tag{4.7}$$

The rate of production ω_i and the term $\left(\sum_{i=1}^{N}h_i\omega_i\right)\Big/\rho$ are given by the equations (2.21) and (2.22). The thermodynamic and kinetic data used here are given in Table 1.

The initial conditions were taken to be

$$y_1(\psi)=\begin{cases}0 & \psi>\psi_0,\\ 0.1259\times10^{-7} & \psi\leqslant\psi_0;\end{cases} \tag{4.8}$$

$$y_2(\psi)=\begin{cases}\dfrac{2}{3} & \psi>\psi_0,\\ 1-0.1259\times10^{-7} & \psi\leqslant\psi_0;\end{cases} \tag{4.9}$$

$$y_3(\psi)=\begin{cases}\dfrac{1}{3} & \psi>\psi_0,\\ 0 & \psi\leqslant\psi_0;\end{cases} \tag{4.10}$$

$$T(\psi)=\begin{cases}300°\mathrm{K} & \psi>\psi_0,\\ 1246.9°\mathrm{K} & \psi\leqslant\psi_0.\end{cases} \tag{4.11}$$

Table 1 Data for Ozone Decomposition

Symbol	Value	Symbol	Value
E_1^f, E_2^f, E_3^f	$24140\ \frac{\text{cal}}{\text{mole}}$	B_4^b	1.88×10^6
E_4^f	$6000\ \frac{\text{cal}}{\text{mole}}$	$B_5^b B_6^b, B_7^b$	2.47×10^2
E_5^f, E_6^f, E_7^f	$117350\ \frac{\text{cal}}{\text{mole}}$	$h_0^{(1)}$	$58675\ \frac{\text{cal}}{\text{mole}}$
E_1^b, E_2^b, E_3^b	0	$h_0^{(2)}$	0
E_4^b	$99210\ \frac{\text{cal}}{\text{mole}}$	$h_0^{(3)}$	$34535\ \frac{\text{cal}}{\text{mole}}$
E_5^b, E_6^b, E_7^b	0	ρ_∞	$1.201\times10^{-3}\ \frac{g}{\text{cm}^3}$
s_1^f, s_2^f, s_3^f	5/2	T_∞	300 °K
s_4^f	5/2	c_{p_∞}	$0.2524\ \frac{\text{cal}}{\text{g-°K}}$
s_5^f, s_6^f, s_7^f	5/2	λ_∞	$9.112\times10^{-5}\ \frac{\text{cal}}{\text{cm-sec}}$
s_1^b, s_2^b, s_3^b	7/2	D_∞	$\frac{\lambda_\infty}{\rho_\infty c_{p_\infty} Le_\infty}$
s_4^b	5/2	M_∞	$16\ \frac{g}{\text{mole}}$
s_5^b, s_6^b, s_7^b	7/2	l_∞	4.203×10^{-3} cm
B_1^f, B_2^f, B_3^f	6.76×10^6	t_∞	5.878×10^{-5} sec
B_4^f	4.58×10^6	l_∞/t_∞	$71.51\ \frac{\text{cm}}{\text{sec}}$
B_5^f, B_6^f, B_7^f	5.71×10^6	p_0	0.821 atm.
B_1^b, B_2^b, B_3^b	1.18×10^2	M_1	$16\ \frac{g}{\text{mole}}$
		M_2	$32\ \frac{g}{\text{mole}}$
		M_3	$48\ \frac{g}{\text{mole}}$

5. Results and Discussion

The solution of the equations (3.1)—(3.2) with boundary conditions (4.4)—(4.7) and initial conditions (4.8)—(4.11) have been obtained for $L_\infty=1$. In the following we describe some results and discuss them.

The DGEAR routine of the IMSL package, which is an adaptation of the package designed by Hindmarsh-Gear, is used for the integration of ODE (3.5). The steady profiles of temperature and concentrations for a fully developed ozone flame are shown in Figures 1—2. Here 29 grid points are used and $\psi_u-\psi_b=12.97$. The flame velocity based on O_2 is $S_u=51.5$cm/sec. Margolis [1] used the method of lines involving collocation with B–splines and obtained $S_u=49.7$ cm/sec, while Bledjian [2] used the method of lines with low order accuracy and got $S_u=54$ cm/sec.

In addition, the flame velocity is senstive to the accuracy of variables, so the appropriate control error must be chosen. In the present case, the control error E is taken to be 10^{-4} in equation (3.9) and 10^{-5} in integration of the ODE.

In order to establish the validity of the movable boundary technique, the fixed

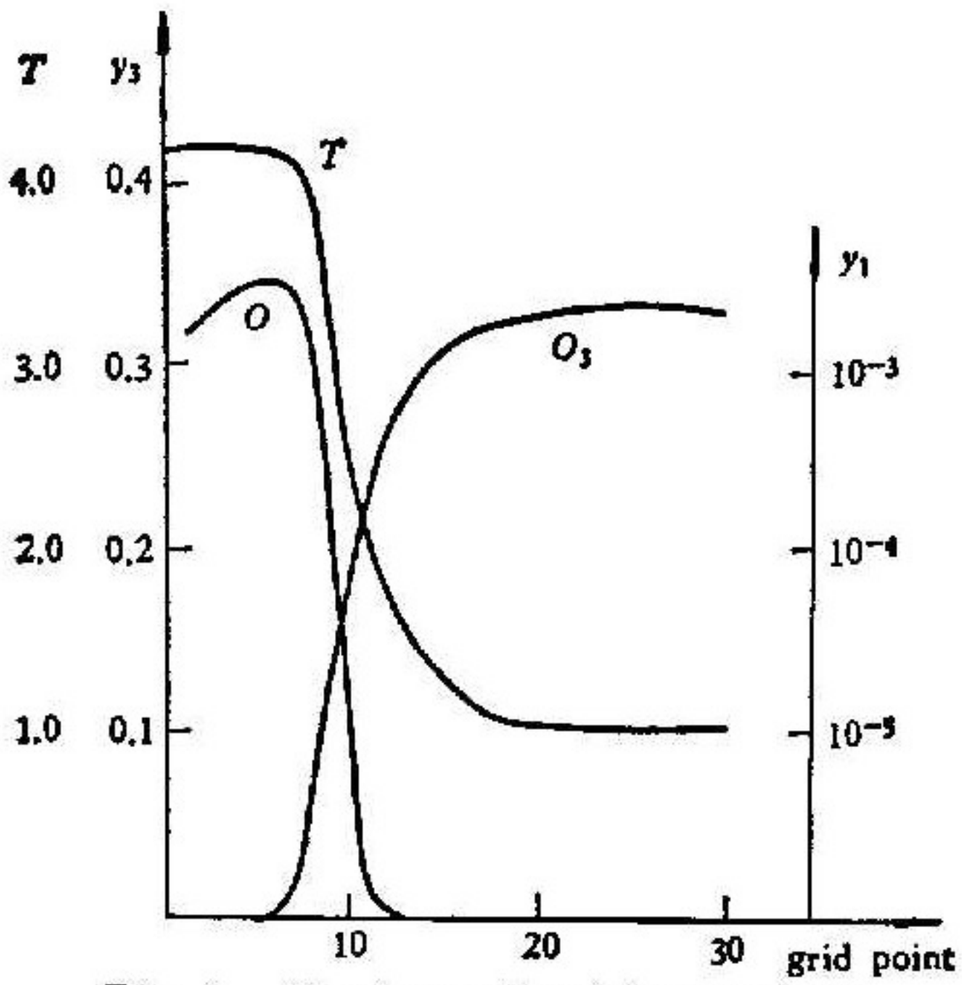

Fig. 1. Steady profile of temperature T and concentrations O, O_3

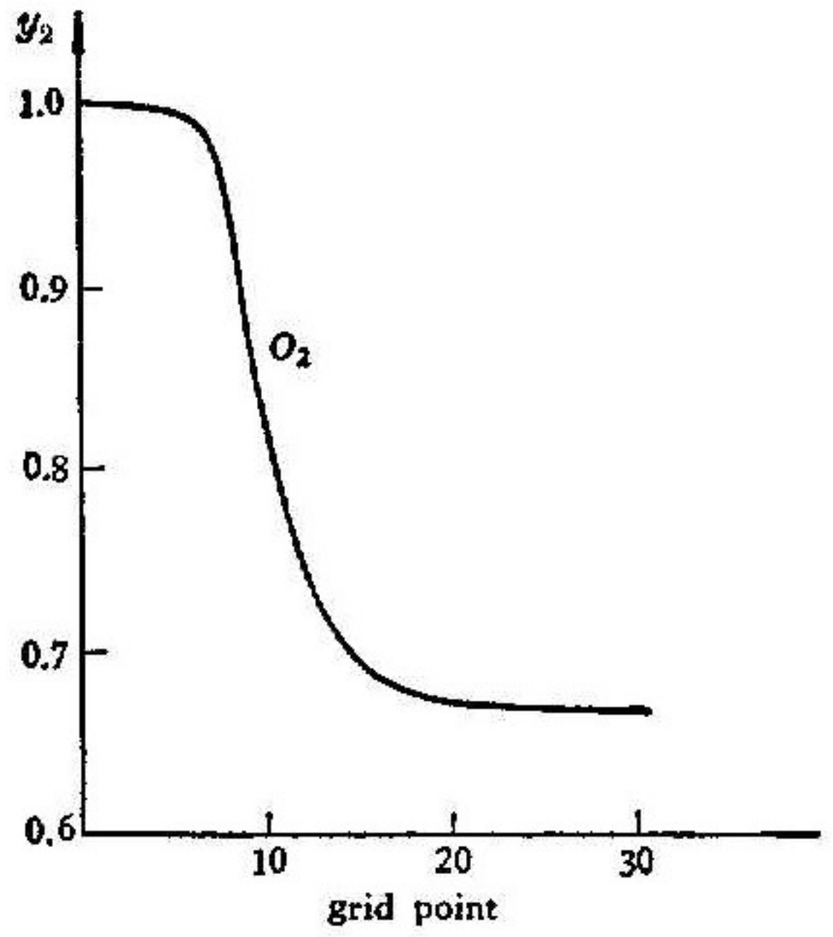

Fig. 2. Steady profile of concentration O_2

boundary is also considered. We take $\psi_u - \psi_b = 50$ and 99 grid points. The time development of the right propagating flame and the profiles of temperature and concentrations are shown in Figures 3—5. The flame velocity is in good agreement with that obtained by movable boundaries. Their deviation is about 0.7%. From this it is seen that the movable boundary technique can significantly reduce grid points; therefore save machine time.

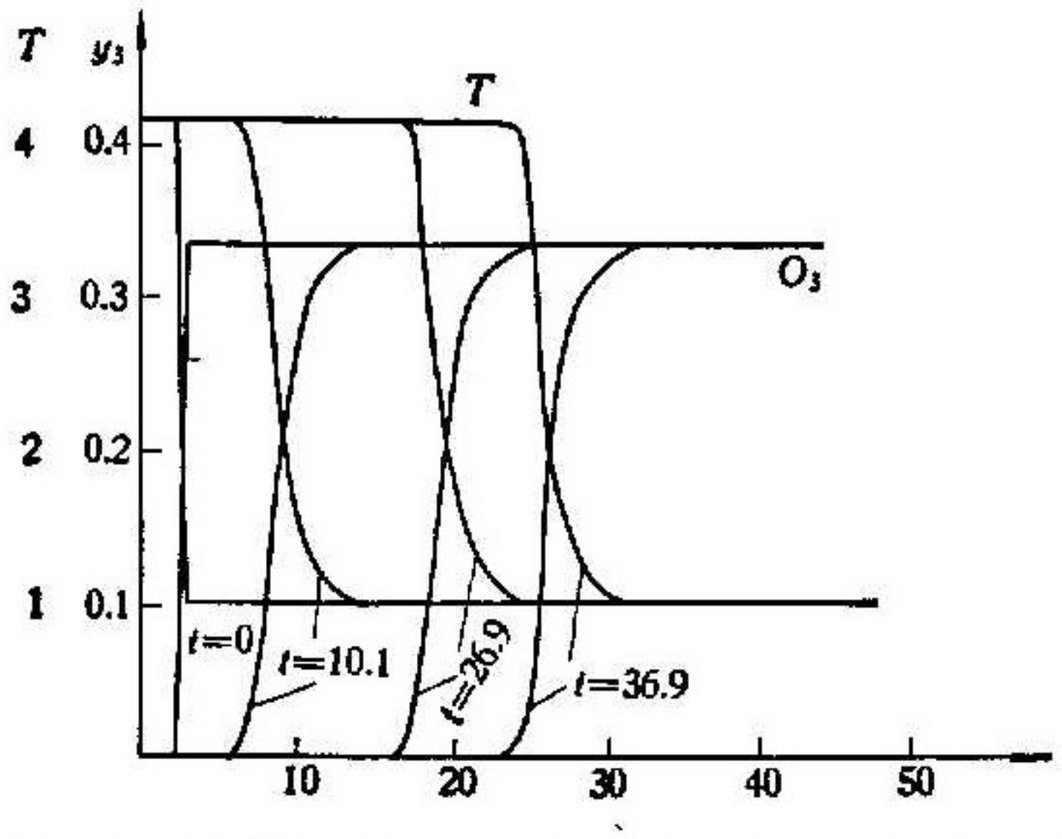

Fig. 3. Profile of temperature T and concentration O_3

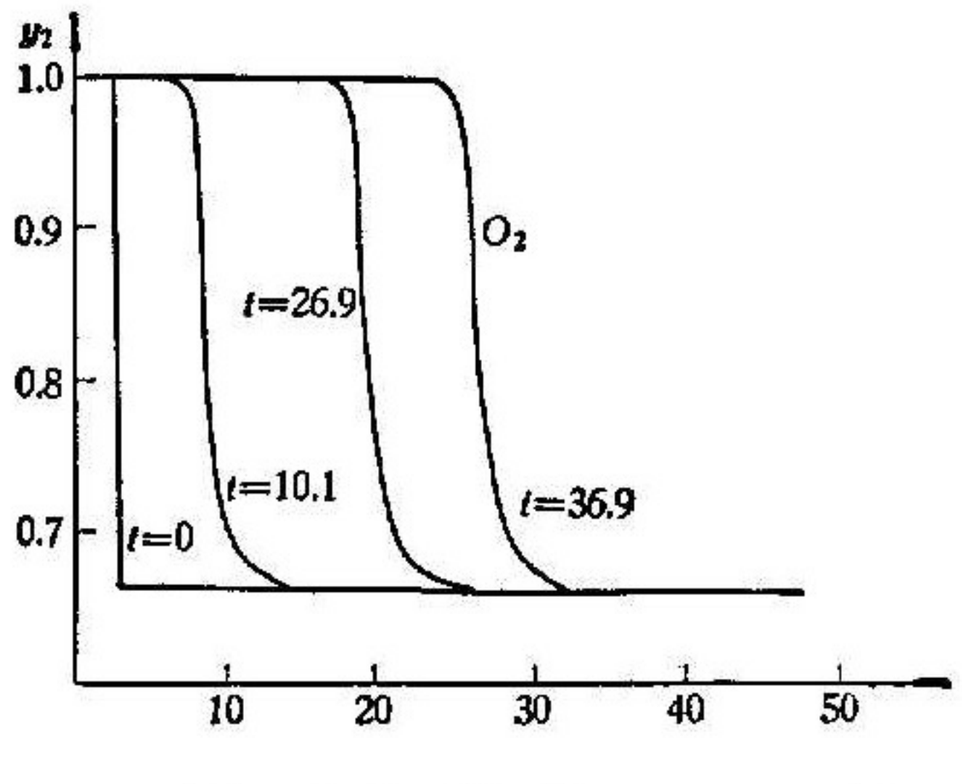

Fig. 4. Profile of concentration O_2

As for the grid points, some tests are made. When grid points are reduced to 19, the results still remain good. The flame velocity is almost the same as that obtained by 29 grid points (the difference between them is only in the fourth decimal). However, when grid points are reduced to 14, the results get worse. The results with 19 grid points are shown in Figures 6—7.

The results are checked in many ways. It is well known that the concentrations must satisfy

$$\sum_{i=1}^{N} y_i = 1.$$

In the present calculation this condition is satisfied very well. Its deviation from 1 is only in the fifth decimal.

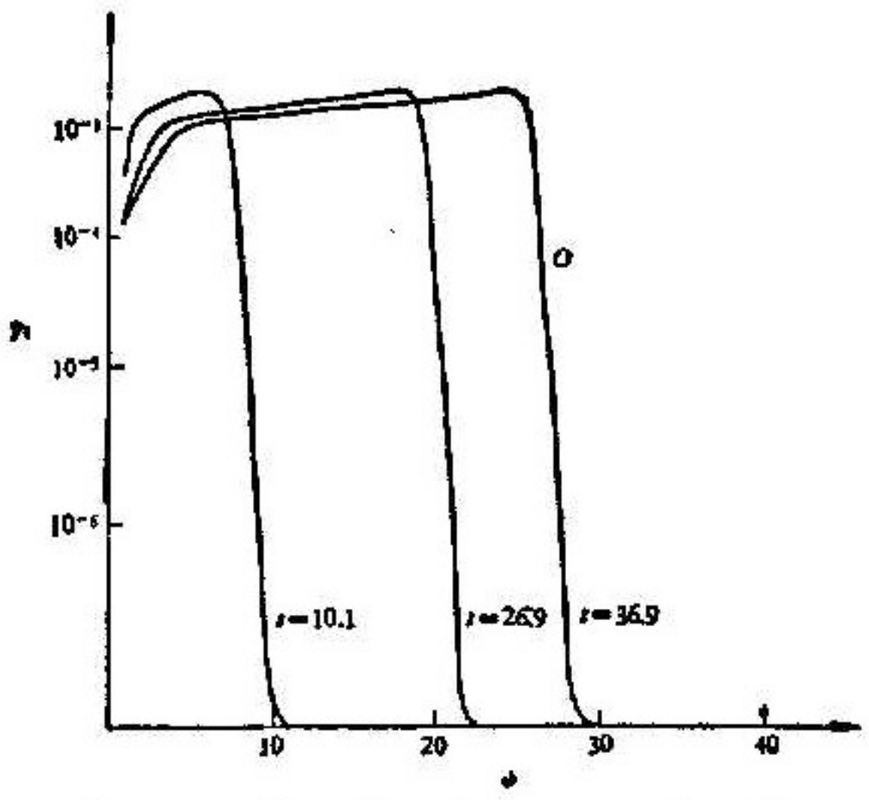

Fig. 5. Profile of concentration O

As mentioned above, a comparison between the flame velocities based on different species can be taken as a check on the results. In our calculation the difference between the flame velocities based on O_2 and O_3 is less than 0.2%.

Finally, a remark has to be made. When using the splitting-up method, one has to decide whether the solution is considered after an $L_D L_C L_C L_D$ sequence or after an $L_C L_D L_D L_C$ sequence. Generally speaking, both yield valid solutions, but there are always some differences between them. In order that the solutions after, an L_D or an L_C step are within a certain tolerance of each other, an additional constraint on the step size is required. Fortunately when the control error mentioned above is used, the solution after an L_C is in good agreement with that after an L_D. The difference between two flame velocities is less than 0.2%,

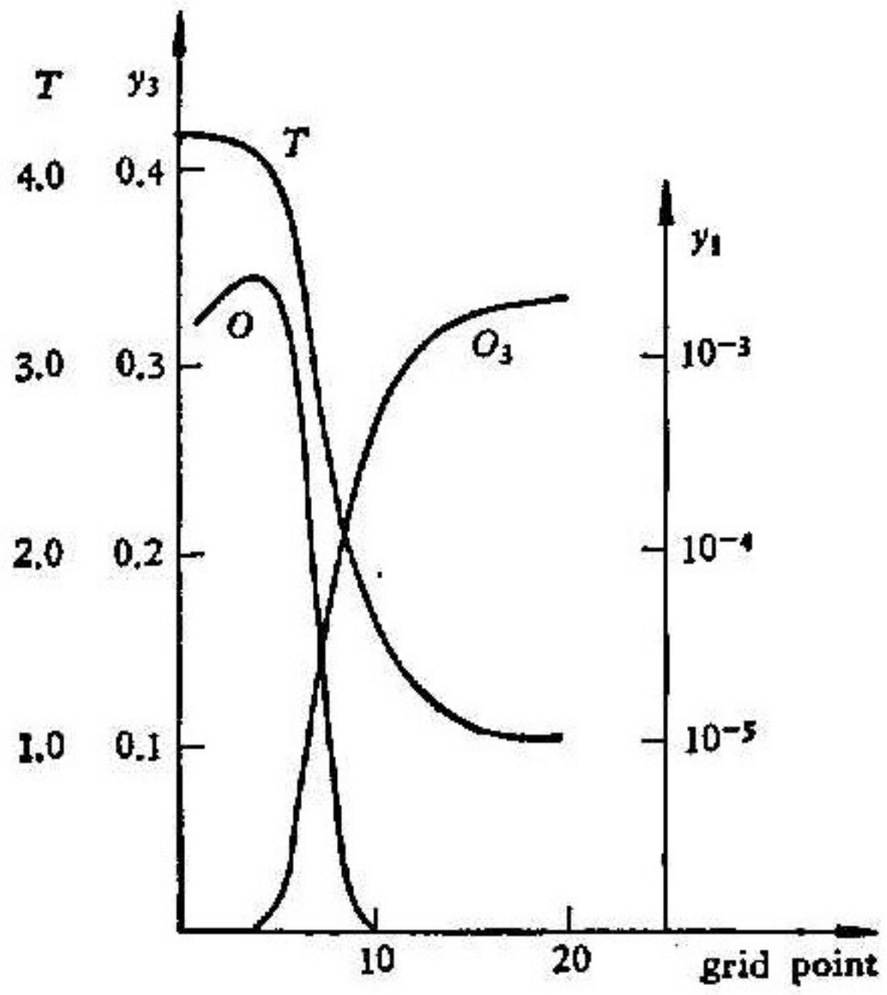

Fig. 6. Steady profile of O, O_3, T

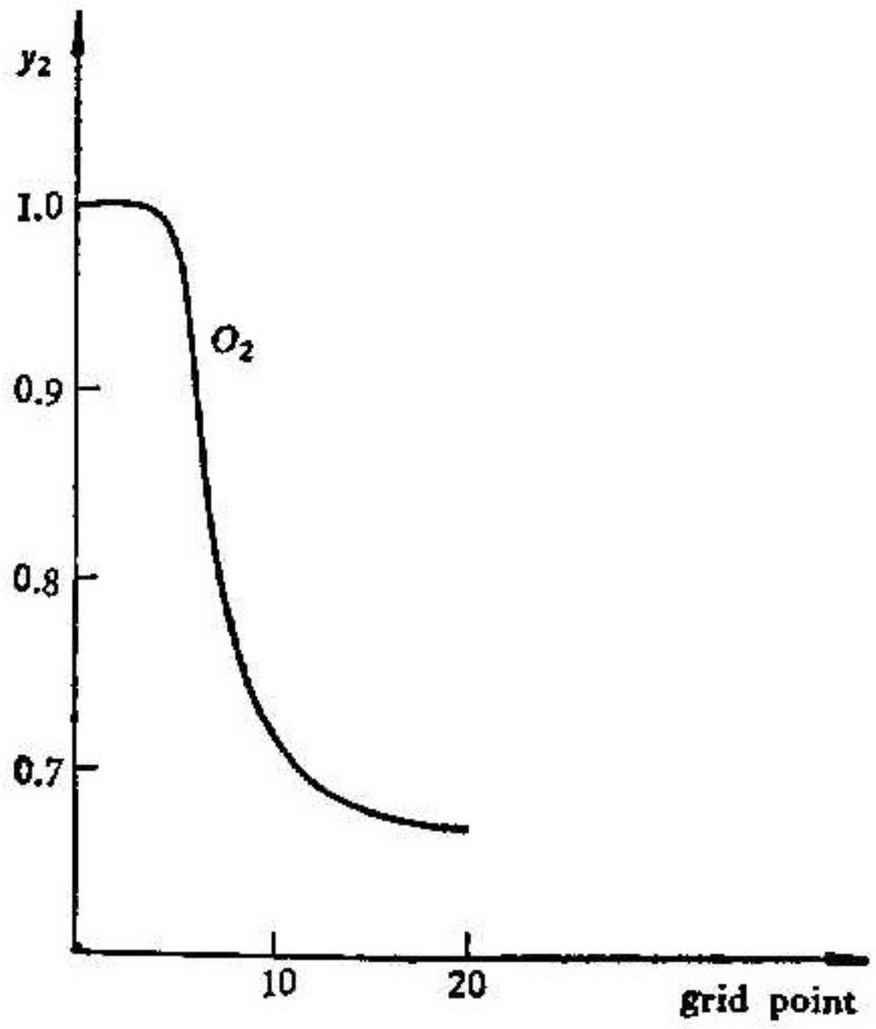

Fig. 7. Steady profile of O_2

Acknowledgments This work was done and supported in part by U. S. Army under Contract No. DAAG29-80-C-0041 during the author's stay at the Mathematics Research Center, University of Wisconsin in 1979—1980.

I would like to thank Professor S. Parter for instructive suggestions and Dr. S. S. Lin for helpful discussions. I also thank Prof. M. C. Shen for his help.

References

[1] S. B. Margolis, Sandia Laboratories, SAND 77—8506, 1977.
[2] L. Bledjian, *Combustion and Flame,* 20 (1973), p. 5.
[3] R. J. Kee and J. A. Miller, Sandia Laboratories, SAND 77—8502, 1977.
[4] A. C. Hindmarsh, Lawrence Livermore Laboratory Report UCID-30130, 1976.
[5] S. S. Lin, Doctoral thesis, University of California, Berkeley, 1979.